Lawrence Berkeley National Laboratory
Recent Work

Title

QUANTITATIVE REGGE EXPRESSIONS+WITH SCALING FOR EXPERIMENTALLY MEASURED FAST n"", K+ INCLUSIVE SPECTRA AND RELATION TO BACKWARD ELASTIC DATA

Permalink

https://escholarship.org/uc/item/3dp8z2kg

Author

Risk, Clifford.

Publication Date

1971-06-01

eScholarship.org Powered by the California Digital Library
University of California

Submitted to
Physical Review

C. Risk

UCRL-20841
Preprint

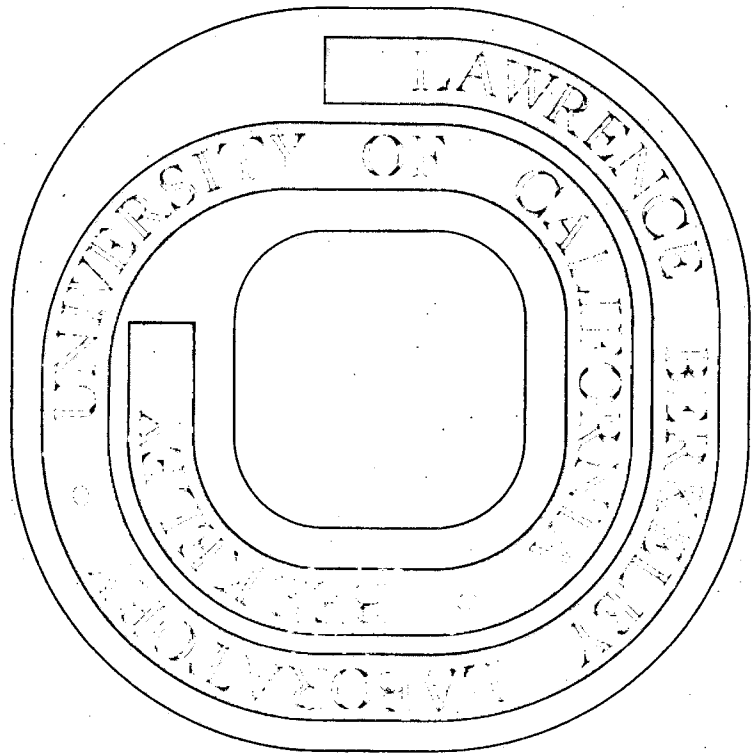

QUANTITATIVE REGGE EXPRESSIONS WITH SCALING FOR EXPERIMENTALLY MEASURED FAST $\pi^{\pm}$, K^{+} INCLUSIVE SPECTRA AND RELATION TO BACKWARD ELASTIC DATA

Clifford Risk

June 21, 1971

AEC Contract No. W-7405-eng-48

TWO-WEEK LOAN COPY

This is a Library Circulating Copy which may be borrowed for two weeks. For a personal retention copy, call Tech. Info. Division, Ext. 5545

DISCLAIMER

This document was prepared as an account of work sponsored by the United States Government. While this document is believed to contain correct information, neither the United States Government nor any agency thereof, nor the Regents of the University of California, nor any of their employees, makes any warranty, express or implied, or assumes any legal responsibility for the accuracy, completeness, or usefulness of any information, apparatus, product, or process disclosed, or represents that its use would not infringe privately owned rights. Reference herein to any specific commercial product, process, or service by its trade name, trademark, manufacturer, or otherwise, does not necessarily constitute or imply its endorsement, recommendation, or favoring by the United States Government or any agency thereof, or the Regents of the University of California. The views and opinions of authors expressed herein do not necessarily state or reflect those of the United States Government or any agency thereof or the Regents of the University of California.

QUANTITATIVE REGGE EXPRESSIONS WITH SCALING FOR EXPERIMENTALLY MEASURED FAST $\pi^{\pm}$, K^{+} INCLUSIVE SPECTRA AND RELATION TO BACKWARD ELASTIC DATA*

Clifford Risk†

Lawrence Radiation Laboratory
University of California
Berkeley, California 94721

and

Department of Physics
University of California
Davis, California 95616

June 21, 1971

ABSTRACT

We represent the spectra for fast π^{+}, π^{-}, K^{+} secondaries in pp collisions in Reggeized forms that describe the experimental data measured at several energies and that scale at high energies. We relate the inclusive amplitudes obtained to backward elastic $\pi^{\pm}p$, $K^{+}p$ scattering and predict both their relative magnitudes and their energy and angle dependence.

* Work supported in part under the auspices of the U.S. Atomic Energy Commission.

† Participating guest at Lawrence Radiation Laboratory, Berkeley.

I. INTRODUCTION

The inclusive reaction $p + p \rightarrow X +$ anything, where X is a specified secondary, offers the simplest probe of the dynamics of particle production processes, and has recently been the subject of experimental and theoretical study. Particle spectra have been measured in pp collisions at energies of 12.4 Ge V/c[1], 19.2 GeV/c[2], and 30 GeV/c[3]. General considerations about the features of the spectra have been proposed by Feynman[4] and Yang[5]; Vander Velde[6] has demonstrated the equivalence of their approaches and shown that the fast secondaries of Ref. 1-3 satisfy their predictions. Calculations of the spectra within specific models - the multi-Regge model[7-9] and the Hagedorn thermodynamic model[10] - have been compared with the measured data.

In this paper we show that the spectra of fast produced $\pi^{\pm}$, K^{+} in pp collisions can be represented by Reggeized expressions that scale at large energy, and that such expressions are intrinsically related to the experimental backward $\pi^{\pm}p$ and $K^{+}p$ elastic two body differential cross-sections. This approach will allow us not only to predict the inclusive fast spectra at high energies, but also to extract the properties of backward elastic cross-sections at lower energies.

Consider first the process $p + p \rightarrow m +$ anything of Fig. 1a, with "m" a produced meson and M^2 representing the remaining secondaries. We will describe those produced $\pi^{\pm}$, K^{+} that emerge with large momentum in the center of mass (cm), and hence with

large positive momentum or small negative momentum in the lab. In a multi-Regge model, these mesons emerge at the end of the multi-peripheral chain, with the incident proton travelling a link down the chain and peripherally scattering with the other incident proton (Fig. 1b). We represent this process with the diagram of Fig. 1c, the cross-section of which is

$$\frac{d^2\sigma}{dtdM^2} = \frac{1}{s^2}\left(\frac{s}{M^2}\right)^{2\alpha(t)} \beta^2(t)\ M^2\sigma_T(M^2). \qquad (1)$$

Here, $\alpha(t)$ is the effective trajectory of the exchanged baryon, $\beta(t)$ is its residue, and $\sigma_T(M^2)$ is the total cross-section for the baryon-baryon scattering. Such an expression was first obtained by Caneschi and Pignotti[7] several years ago on the basis of multi-Reggeism. Recently, Peccei and Pignotti[12] have further studied the experimental consequences of (1).

We organize the paper as follows. In Sec. II we discuss the spectra predicted by (1), and its approach to a scaling limit. In Sec. III we obtain quantitative expressions of the type (1) for the $\pi^{\pm}$, K^+ spectra from the 19.2 GeV/c data. In Sec. IV we test the scaling predictions of (1) by comparing with the 12.4 GeV/c and 30 GeV/c data. The shape of the fast backward spectra predicted by (1) should be independent of the incident particle, and in Sec. V we compare (1) with the π^- fragmentation of the proton in K^+p collisions at 12.4 GeV/c. In Sec. VI we discuss the relation between the inclusive inelastic process of (1) and the elastic backward meson-proton differential cross-sections, and we use this relation to predict energy dependence, angle

dependence, and relative normalization of the three processes. Sec. VII contains remarks about the K^-, $\bar{p}$ and p spectra.

II. SPECTRUM PREDICTED BY EQ. (1)

The momentum spectrum predicted by (1) will be given by

$$d^3\sigma = \frac{d^3p}{E}\ \frac{2mp_o}{\pi}\ \frac{d^2\sigma}{dtdM^2} \qquad (2)$$

Here, p and E are the momentum and energy of the secondary, p_o is the incident beam target. We can express (2) in terms of the longitudinal and transverse momentum components p_L, p_T of the secondary in the cm by using

$$t = m^2 + \mu^2 + 2(\bar{p}_o p_L - \bar{E}_o E), \qquad (3a)$$

$$M^2 = 4\bar{E}_o^2 - 4\bar{E}_o E + \mu^2; \qquad (3b)$$

μ is the mass of the secondary, and $\bar{p}_o$, $\bar{E}_o$ are the cm momentum and energy of the incident particle. When p_L and $\bar{p}_o$ are both large, we introduce $x = p_L/\bar{p}_o \sim E/\bar{E}_o$, and t, M^2 become

$$t = m^2(1-x) + \mu^2 - (p_T^2 + \mu^2)/x \qquad (4a)$$

$$M^2 = s(1-x) \qquad (4b)$$

The spectrum is then given by

$$d^3\sigma = \frac{d^3p}{E}\ \frac{(1-x)^{1-2\alpha(t)}}{\pi}\ \beta^2(t) \qquad (4c)$$

$$= \frac{d^3p}{E}\ f(x, p_T) \qquad (4d)$$

where $f(x, p_T)$ is the Feynman scaling function.

In the lab system, the expressions for t, M^2 became

$$t = m^2 + \mu^2 - 2(p_o p_L - E_o E) \to m^2(1 - R) + \mu^2 - (p_T^2 + \mu^2)/R \quad (5a)$$

$$M^2 = (E_o + m - E)^2 - p_o^2 - p^2 + 2p_o p_L \to s(1-R) \quad (5b)$$

where $R = p/p_o \approx p_L/p_o$, as introduced by Vander Velde[6], and the spectrum becomes

$$d^3\sigma = \frac{d^3p}{E} f(R, p_T). \quad (5c)$$

Finally, we can derive the expression for slow secondaries in the lab (backward fast secondaries in the cm) by writing t, M^2 relative to the target:

$$t = m^2 + \mu^2 - 2mE \quad (6a)$$

$$M^2 = (E_o + m - E)^2 - p_o^2 - p^2 + 2p_o p_L \to s[1 - (E - p_L)/m] \quad (6b)$$

$$d^3\sigma = \frac{d^3p}{E} \frac{1}{\pi} \left[1 - (E-p_L)/m\right]^{1-2\alpha(t)} \beta^2(t) \quad (6c)$$

Eq. (6c) depends only on p_L, p_T and is independent of p_o, as conjectured by Yang[5,6].

III. QUANTITATIVE EXPRESSIONS FOR THE SPECTRA

To derive quantitative expressions for the secondary spectra, first we compare Eq. (1) with the 19.2 GeV/c data (Fig. 2). We cut the data at fixed M^2 (Fig. 3) and plot against t. This gives Fig. 4(a,b,c). Perhaps the most interesting features of the data are the sharp forward t- dependence and the shrinking diffraction behavior as M^2 decreases (or the Regge sub-energy s/M^2 increases).

If Eq. (1) is to represent the data, then a plot of the cross-section at fixed t against M^2 on a log-log graph should give straight lines of slope $2\alpha(t) - 1$. These plots are shown in Fig. 5 (a,b,c). The π^+ cross section in Fig. 5(a) shows the most dramatic Regge behavior, with straight lines over as much as 2 1/2 decades in the data. The π^- and K^+ data also show Regge behavior over $M^2 < 20$.

The Regge trajectories $\alpha(t)$ can now be evaluated from the slopes of Fig. 5 (we take $\sigma_T \equiv 1$), and they are graphed in Fig. 6. The relatively low intercepts are at first surprising, but we shall see that this corresponds to the relatively fast fall in the backward elastic processes in the intermediate energy range (p_o = 2 - 4 GeV/c).

Next we assume the cross-section does take the form (1) and set $s = 37.8\ (\text{GeV})^2$ - the s-dependence will be verified by comparring (1) with spectra at other energies. We solve for the residues $\beta^2(t)$, and this gives Fig. 7.

Collecting these results, we compare (2) with the experimental data in Fig. 2.

1. π^+ spectra: Eq. (2) adequately represents the data for $R > 0.4$, except for the structure at $p = 14$ GeV/c. For $R < 0.4$, we expect the diagram of Fig. 2(e) (internal pionization) to contribute to the spectrum, and Eq. (2) falls below the data.

2. π^- spectra: Eq. (2) represents the data for $R > 0.4$. Note that the π^- spectrum at 12.5 mrad falls by 3 decades from $p = 4.5$ GeV/c to $p = 16$ GeV/c, while the π^+ spectrum falls only 2 decades. It is this relatively rapid fall-off in the fast π^- spectrum in the Regge region that leads to the low value of $\alpha_\Delta(t)$, and this is related to the relatively rapid fall-off in the $\pi^- p$ backward elastic cross-section (Sec. VI).

3. K^+ spectra: Eq. (2) represents the data for $R > 0.5$, except for the 12.5 mrad data, which gives a p_T dependence at $p_T \sim 0$ that becomes very broad for $p < 12$ GeV/c. Generally, the momentum dependence of K^+ spectra is similar to that of the π^+, and this leads to the similarity of their trajectories in Fig. 6.

In all cases, Eq. (2) overestimates the data for $R \gtrsim 0.98$ as p approaches the kinematical limit at $p \sim 19$ GeV/c, because the condition that $\sigma_T(M^2) \to 0$ at threshold has not been used.

IV. COMPARISON WITH 12.4 GeV/c AND 30 GeV/c DATA

The trajectories and residues of Fig. 6,7 have been obtained from Eq. (2) by fixing $s = 37.8$ (GeV)^2. To test the energy dependence of (2), we compare our quantitative expressions with the data at 12.4 GeV/c and 30 GeV/c in Fig. 8.

1. π^+ data (Fig. 8a): The data at $p_T^2 = 0.22$ (GeV/c)^2 is adequately predicted for $x > 0.4$. The data at $p_T^2 = 0.43$ (GeV/c)^2 stops at somewhat small x for a comparison. In Fig. 8c, the prediction at 15 mrad is adequate for $R > 0.2$.

The dashed lines in Fig. 8(a,c) represent extrapolations of Fig. 6 to the range of $t < -1.2$ (GeV)^2, where Ref. 1 had no data. These extrapolations were obtained by linearly extending $\alpha(t)$ and taking $\beta_N^2(t)$ as listed in Table 1. Other extrapolations - such as a flattening $\alpha(t)$ - could have been used; there is too little data for a unique extrapolation and we report our result only as a guide.

2. π^- data: The features of the π^- predictions Fig. 8 (b,c) are similar to those of the π^+, except that at both energies they are on the average 50% above the data. This result was also obtained by Vander Velde[6] in his scaling analysis of the data and represents possible differences in the overall normalization of the different experiments. In counter experiments, such discrepancies are possible[12].

V. COMPARISON WITH π^- FROM Kp DATA

The spectra of the fast π^- that are backward in the cm should be the same in Kp collisions as in pp collisions. In the multiperipheral model this comes about from these π^- being emitted at the proton end of the chain and hence having a spectrum independent of the beam particle. To test the present model with this conjecture, we compare the prediction of (2) with the spectrum of Ko and Lander[13] in Fig. 9. The agreement is reasonable. In particular, note that Eq. (2) describes the π^- mesons with small p_T to a small value of x, $x \sim 0.2$, but π^- mesons with large p_T only up to $x \sim 0.5$. As discussed in Ref. 9, this occurs because Figs. 1(b,c) give rise to the forward scattered mesons at small p_T, whereas Fig. 1(e) gives rise to mesons at larger values of p_T. Hence the extrapolation of Eq. (2) to small x when p_T is small is expected to be good.

VI. RELATION OF INCLUSIVE SPECTRA TO TWO BODY ELASTIC BACKWARD CROSS SECTIONS

The multiperipheral diagrams of Fig. 1 impose a direct relation between the inclusive inelastic process and the elastic backward process. If we neglect the off-mass shell effects of the exchanged baryon in Fig. 1(b), then we are led to represent the two-body process of Fig. 1(d) as

$$\frac{d\sigma(s,u)}{du} = \frac{c}{s^2} s^{2\alpha(u)} \beta^2(u) \tag{8}$$

c is a constant. That is, we expect generally that if the two-body process is represented by

$$\frac{d\sigma}{du}(s,u) = \frac{c}{s^2} \left| A(s,u) \right|^2 , \tag{9a}$$

then the inclusive process is given by

$$\frac{d^2\sigma(s,t,M^2)}{dt dM^2} = \frac{1}{s^2} \left| A\left(\frac{s}{M^2},t\right) \right|^2 M^2 \sigma_T(M^2). \tag{9b}$$

Over what energy range should we expect to predict the two-body data? In the Allaby data, $s = 37.8\ (\text{GeV})^2$, and the representations obtained have adequately described the inclusive data for $M^2 = 6 - 20\ (\text{GeV})^2$. Therefore, we are led to predict the two-body data with Eq. (8) for $s \sim 2 - 8\ (\text{GeV})^2$; this corresponds to the intermediate energy range extending from just above the $\Delta(1236)$ resonance region to the onset of the high energy pure Regge region.

To test this relation, we have evaluated Eq. (8) for the three backward elastic processes - π^+p, π^-p, K^+p. In this comparison, we normalize one process (π^-p) to the data and then predict the normalizations of the remaining two processes and the s and u dependence of all three.

In Fig.10(a,b,c) we compare the predicted backward elastic cross-section at 180° with the experimental data as a function of energy. In Fig.10(a), the π^+ prediction represents an average of the backward two-body behavior. The absence of the N^* resonances at 1525, 1670, 1688 and 1700 GeV forces the π^+p cross-section to a low average value in the range $p_\pi \sim 1 - 2$ GeV/c; its average value is one to two times larger than the π^-p cross-section. At larger p_π, $p_\pi \sim 4 - 5$ GeV/c, the π^+p process is ten times larger than the π^-p process. As discussed in Ref. 9, it is this relatively faster fall-off in the π^-p process that leads to the low position of the α_Δ in Fig. 7. (At large p_π beyond the resonance region, $p_\pi > 4$ GeV/c, the canonical trajectories dominate the π^-p cross section and Eq. (8) undercuts the data.) Similarly, for $p_K > 1.5$ GeV/c, the backward K^+p process has an energy dependence similar to the π^+p; this leads to the inclusive π^+, K^+ spectra having similar momentum dependence (Fig. 2) and hence similar trajectories (Fig. 7).

If we now turn to small values of p_π in Fig.10(a), $p_\pi \sim 1$ GeV c, we see that the theoretical $d\sigma/d\omega$ undercuts the structure at the $\Delta(1236)$ resonance. This corresponds in Fig. 2(a) to the bump in the π^+ spectrum at $p \sim 6$ GeV/c, which similarly

lies above the background predicted by the theoretical distribution. (In Fig. 8(c) this bump occurs at the scaled value $p \sim 9$ GeV/c.) A similar undercutting in the K^+ data in the resonance region occurs in Fig. 2(c) and Fig.10(c).

We can also compare the angular dependence predicted with the experimental data. In Fig.10(d) we see that the π^+p differential cross-section predicted by Eq. (8) is in reasonable agreement with the data. The prediction for the π^-p data in Fig.10(e) represents an average to the experimentally measured cross-section. In Figs. 10(f,g) there is a reasonable agreement for the K^+p data.

VII. THE K^-, $\bar{p}$, AND p SPECTRA

The spectra for K^-, $\bar{p}$, and p secondaries are very different than the $\pi^\pm$, K^+ secondaries. We expect few fast K^-, because the backward K^-p elastic cross-section falls very rapidly in the intermediate energy range. An analysis of the type performed here should lead to a low effective trajectory, with an intercept ~ -4.

Similarly, we expect no fast $\bar{p}$ at all because of the absence of double baryon exchange in Fig. 1(c).

The proton spectrum is a special case. If we plot the data at fixed M^2 against t, we obtain Fig. 11(a), we again obtain sharp forward peaking at small t; but in contrast to the $\pi^\pm$, K^+ spectra, there is no shrinking diffraction peak. This can be seen in Fig. 11(b), where we plot the data a fixed t against M^2 on a log- plot. The indication of straight lines suggests a representation of the form

$$\frac{d^2\sigma}{dtdM^2} \sim \frac{e^{a(t)M^2/s}}{s} \qquad (10)$$

By performing this analysis on the data at the other two energies of Ref. 2,3, we have found that the exponent of Eq. (10) does take the scaling form indicated[18]. These results will be reported elsewhere.

ACKNOWLEDGEMENTS

I am very grateful to Professor Richard Lander for the hospitality extended to me at Davis during the present year. I am also grateful to Professor Lander and Dr. Winston Ko for fruitful discussions leading to completion of the work, and to members at Davis of the Physics 129 seminar for stimulating interactions. Discussions with Professor J. Ball, Dr. W. Swanson, Professor L. Stevenson and Professor V. Chung are appreciated. Professor G. Chew and Professor J. D. Jackson are warmly thanked for the hospitality of Lawrence Radiation Laboratory.

The present work has greatly benefitted from a collaboration with Dr. J. H. Friedman involving development of phenomenological models for inelastic processes.

TABLE 1

PARAMETERS REPRESENTING THE DATA

$\alpha_N(t)$	=	$-1.35 + 1.25t$	$t > 0$
		$-1.35 + 0.35t$	$t < 0$
$\alpha_\Delta(t)$	=	$-1.9 + 1.25t$	$t > 0$
		$-1.9 + 0.75t$	$t < 0$
$\alpha_\Lambda(t)$	=	$-1.15 + 1.5t$	$t > 0$
		$-1.15 + 0.75t$	$-0.4 < t < 0$
		$-1.25 + 0.5t$	$t < -0.4$
$\beta_N^2(t)$	=	$50\ e^{1.3t}$	$t > -1.2$
		$10.5\ e^{0.345(t + 1.2)}$	$-4. < t < -1.2$
		$4.$	$t < -4.$
$\beta_\Delta^2(t)$	=	$35\ e^{1.03(t + 0.2)}$	$t > -0.2$
		$35\ e^{0.47(t + 0.2)}$	$-1. < t < -0.2$
		$35\ e^{-0.38}$	$t < -1.$
$\beta_\Lambda^2(t)$	=	$7.4\ e^{1.05t}$	$t > -0.5$
		$4.39\ e^{0.69(t + 0.5)}$	$t < -0.5$

The $\beta_\Delta^2(t)$ is based on the 19.2 GeV/c data. We recommend an extra factor of 0.6 to bring agreement with the 12.4- and 30-GeV/c data. The constant "c" in Eq. (8) is 30.

FOOTNOTES AND REFERENCES

1. C. W. Akerlof, et al., Phys. Rev. D3, 645 (1971).

2. J. V. Allaby, et al., CERN preprint 70-12, April, 1970 (unpublished).

3. E. W. Anderson, et al., Phys. Rev. Letters 19, 198 (1967).

4. R. P. Feynman, in Proceedings of the Third International Conference - High Energy Collisions, Stony Brook, 1969, edited by C. N. Yang, et al. (Gordon and Breach, New York, 1969).

5. J. Benecke, T. T. Chou, C. N. Yang, and E. Yen, Phys. Rev. 188, 2159 (1969).

6. J. C. Vander Velde, Phys. Rev. Letters 32B, 501 (1970).

7. L. Caneschi and A. Pignotti, Phys. Rev. Letters 19, 198 (1967).

8. L. Caneschi, D. E. Lyon, Jr., and Clifford Risk, Phys. Rev. Letters 25, 774 (1970).

9. Clifford Risk and Jerome H. Friedman, UCRL-20 199, March 1971 (to be published in Phys. Rev. Letters).

10. J. Ranft, Phys. Rev. Letters 33B, 481 (1970).

11. R. D. Peccei and A. Pignotti, Phys. Rev. Letters 26, 1076 (1971).

12. J. Vander Velde and D. Smith (private communications).

13. W. Ko and R. Lander, Phys. Rev. Letters 26, 1064 (1971); 26, 1284 (1971).

14. The experimental data of Fig.10 have been taken from the following: Fig. 13(a), (b) - from Ref. 15; Fig.10(c) - from tabulation of Ref. 16; Fig.10(d,e) - Ref. 17; Fig.10(f) - Ref. 16.

15. H. L. Anderson, et al., Phys. Rev. 3D, 1536 (1971).

16. Particle Data Group, UCRL-20000 K^+N, September, 1969 (unpublished)

17. A. S. Carroll, et al., Phys. Rev. Letters 20, 607 (1968).

18. The form of Eq. (10) arises from the contribution to the proton spectrum from Fig. 1(b) (J. Ball, private communication). These protons have become inelastic and are scattered into larger angles. In Ref. 9, this portion of the spectrum was described by the sum of the contribution from Fig. 1(b)and the diagram for the fast proton emerging at the end of the multi-Regge chain.

FIGURE CAPTIONS

Fig. 1. Diagrams for fast mesons. (a) Diagram for a produced meson. (b) Multi-Regge representation of (a) for a fast meson. (c) Multi/Regge diagram used in this paper. (d) Diagram for backward elastic meson-proton scattering. (e) Meson produced internally in the multi-Regge model.

Fig. 2. Spectra for fast $\pi^{\pm}$, K in pp collisions at 19.2 GeV/c. The solid lines are the theoretical representation of the data obtained in this paper.

Fig. 3. Cuts on the data of Fig. 2(a) at fixed M^2. The curved lines are from Ref. 1.

Fig. 4. The data of Fig. 2 replotted at fixed M^2 against t. Dots represent the interpolations of the data of Fig. 2 and Fig. 3.

Fig. 5. The data of Fig. 4 replotted at fixed t against M^2.

Fig. 6. Effective trajectories obtained from the slopes of Fig. 5; α_N, α_Δ, α_Λ refer to the trajectories for the π^+, π^-, and K spectra respectively.

Fig. 7. Residues $\beta^2(t)$ obtained from Figs. 4, 6.

Fig. 8. Predictions of Eq. (2) for the $\pi^{\pm}$ data: (a,b) at 12.4 GeV/c; and (c) at 30 GeV/c.

Fig. 9. Predictions of Eq. (2) for the π^- data from K^+p collisions at 11.8 GeV/c. To account for the known p_T distribution in each bin, the theoretical curves are calculated at p_T = 0.13, 0.3, 0.48, 0.68, 0.88 GeV/c.

Fig. 10. Predictions of Eq. (8) for backward π^+p, π^-p, K^+p elastic differential cross-sections. (a,b,c) - momentum dependence at 180°. (d,e,f,g) - angle dependence at fixed momentum.

Fig. 11. The proton spectra at 19.2 GeV/c. Plotted (a) at fixed M^2 against t; (b) at fixed t against M^2.

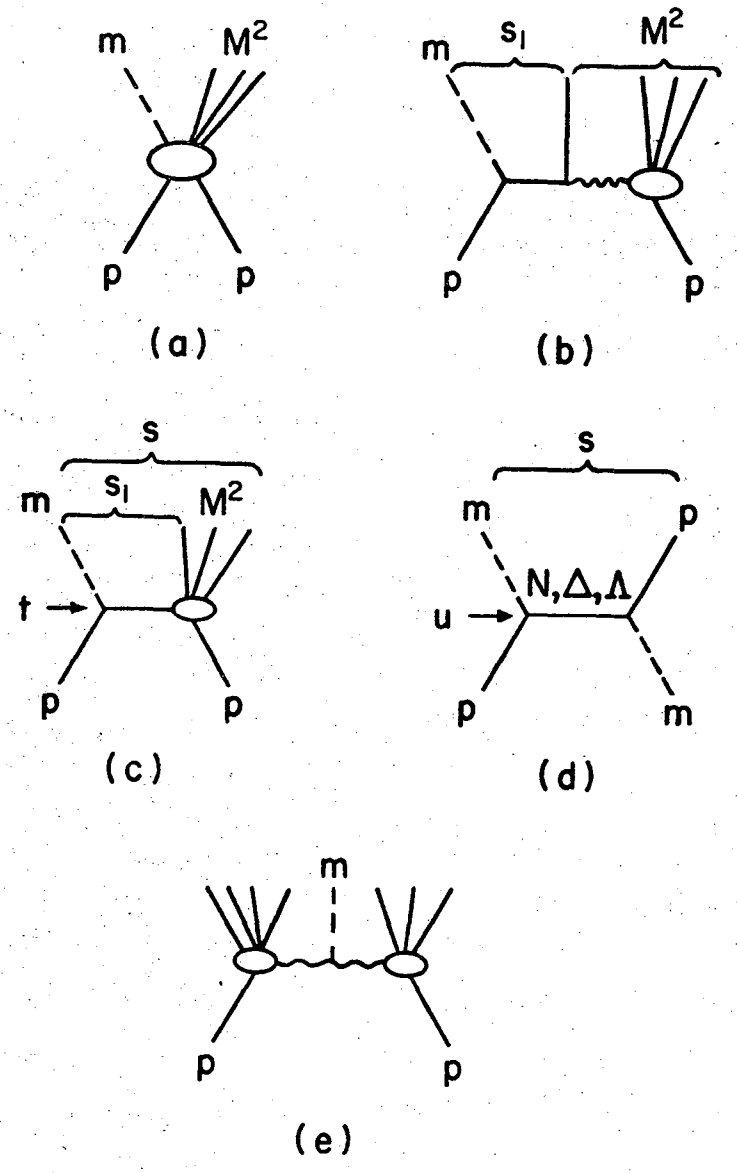

XBL716-3685

Fig. 1

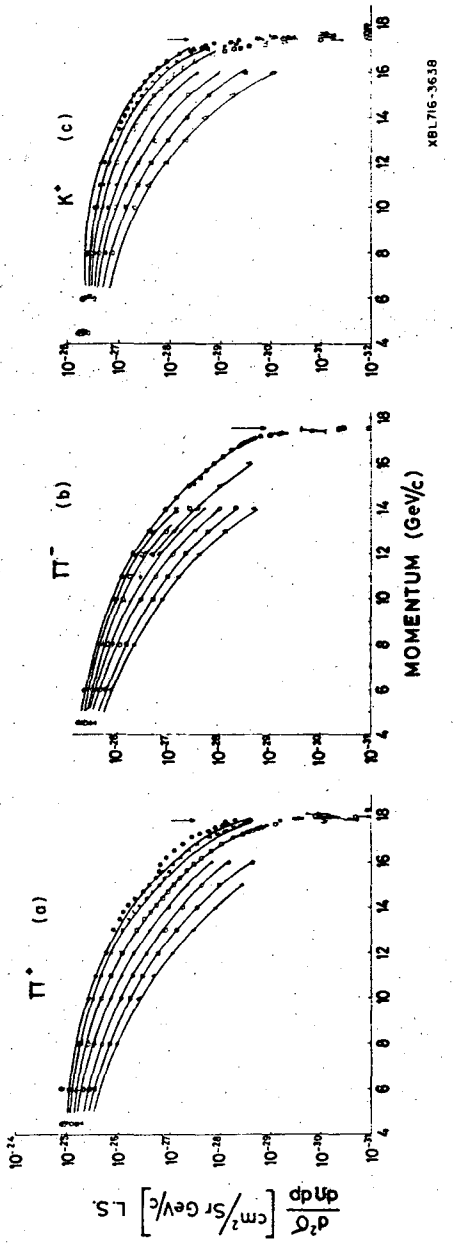

Fig. 2

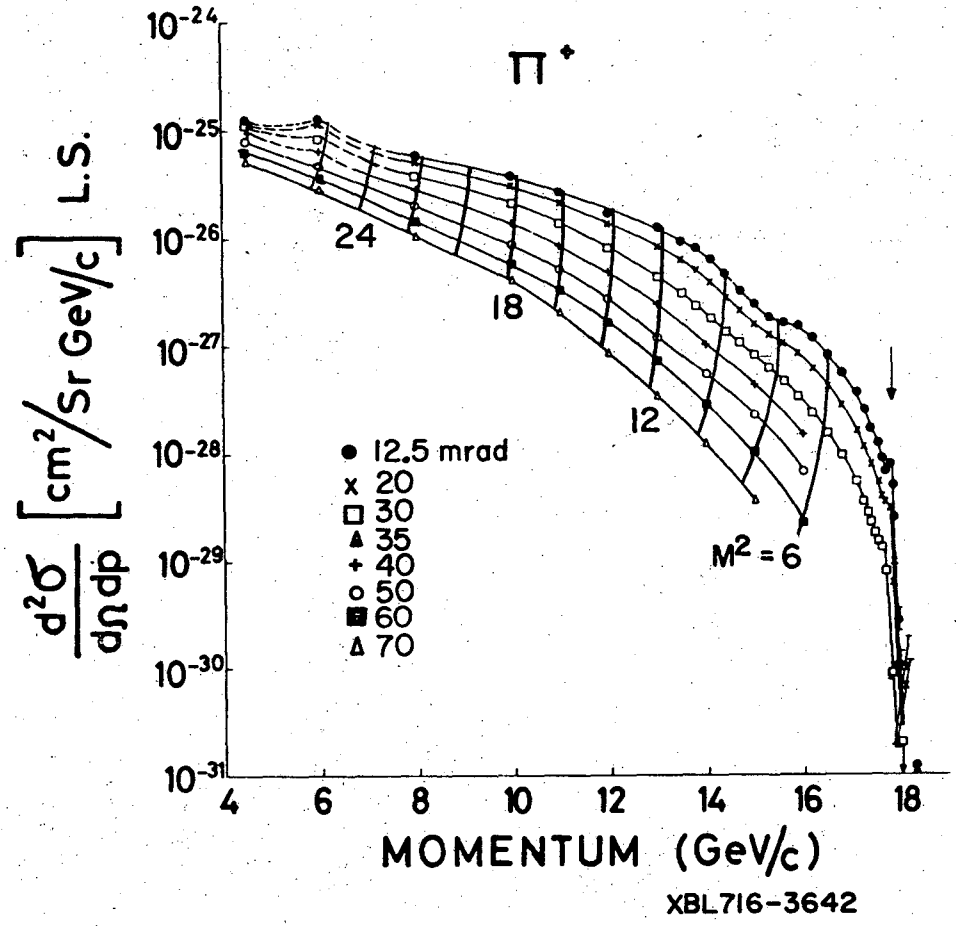
Π⁺
$\frac{d^2\sigma}{d\Omega dp}$ [cm²/Sr GeV/c] L.S.
10⁻²⁴
10⁻²⁵
10⁻²⁶
10⁻²⁷
10⁻²⁸
10⁻²⁹
10⁻³⁰
10⁻³¹
24
18
12
M² = 6
● 12.5 mrad
x 20
□ 30
▲ 35
+ 40
o 50
■ 60
Δ 70
4 6 8 10 12 14 16 18
MOMENTUM (GeV/c)
XBL716-3642

Fig. 3

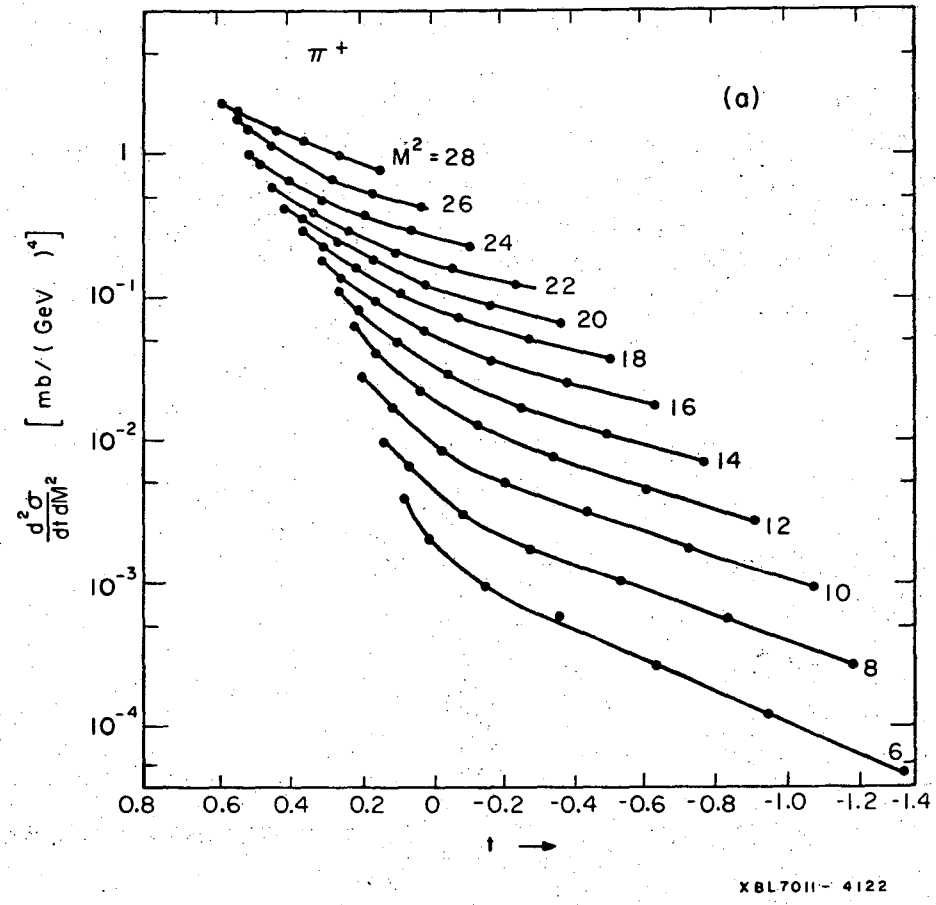
π⁺
(a)
$\frac{d^2\sigma}{dtdM^2}$ [mb/(GeV)⁴]
M² = 28
26
24
22
20
18
16
14
12
10
8
6
1
10⁻¹
10⁻²
10⁻³
10⁻⁴
0.8 0.6 0.4 0.2 0 -0.2 -0.4 -0.6 -0.8 -1.0 -1.2 -1.4
t →
XBL7011-4122

Fig. 4a

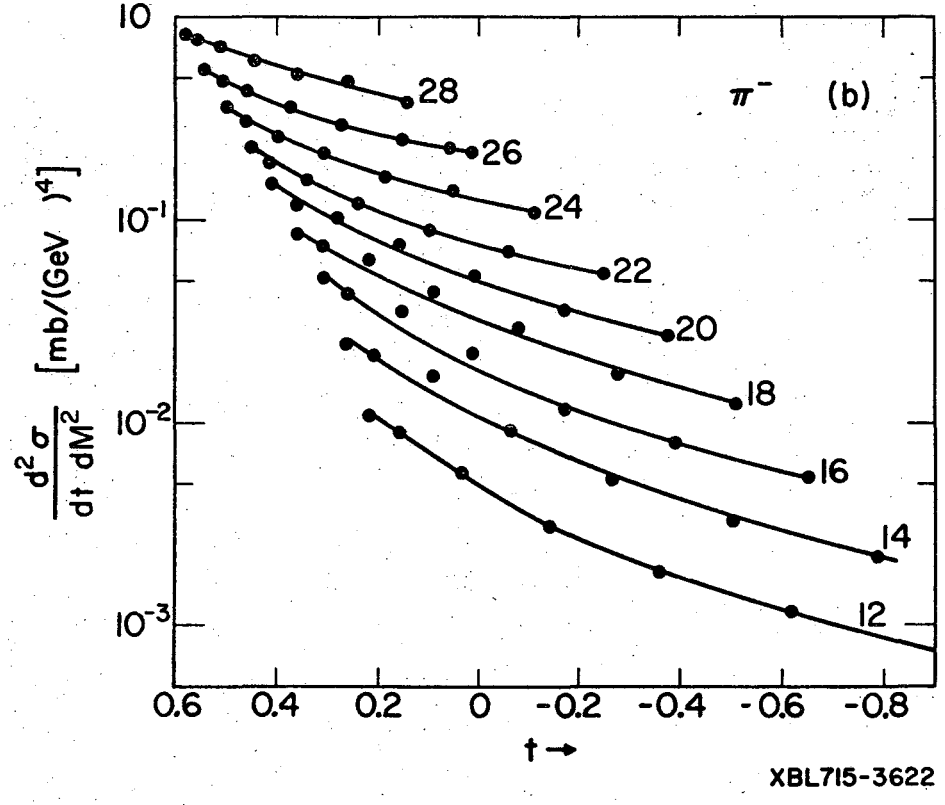
10
10^{-1}
10^{-2}
10^{-3}
$\frac{d^2\sigma}{dt\ dM^2}$ [mb/(GeV)^4]
π^- (b)
28
26
24
22
20
18
16
14
12
0.6 0.4 0.2 0 -0.2 -0.4 -0.6 -0.8
t →
XBL715-3622

Fig. 4b

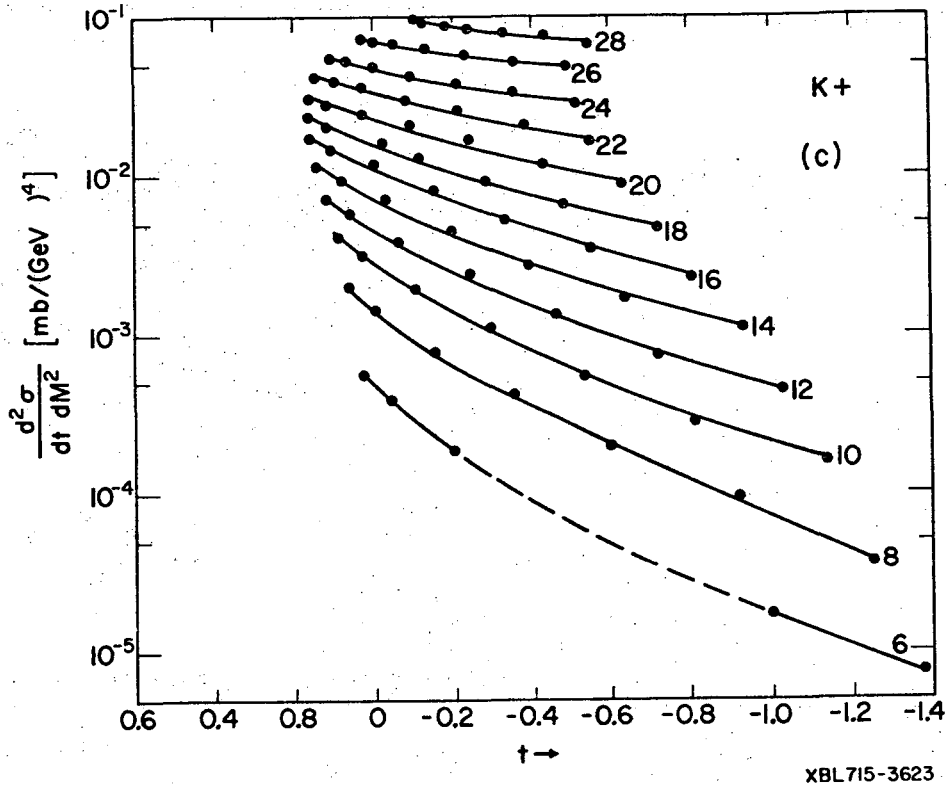
10^{-1}
10^{-2}
10^{-3}
10^{-4}
10^{-5}
$\frac{d^2\sigma}{dt\ dM^2}$ [mb/(GeV)^4]
K+
(c)
28
26
24
22
20
18
16
14
12
10
8
6
0.6 0.4 0.8 0 -0.2 -0.4 -0.6 -0.8 -1.0 -1.2 -1.4
t →
XBL715-3623

Fig. 4c

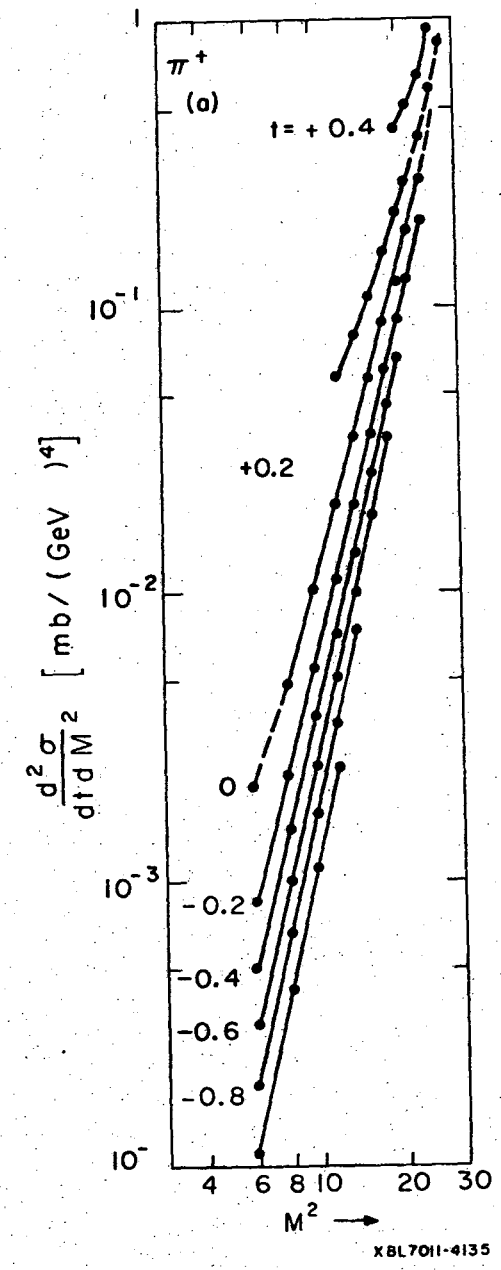
π+
(a)
t = + 0.4
+0.2
0
-0.2
-0.4
-0.6
-0.8
1
10⁻¹
10⁻²
10⁻³
10⁻
4 6 8 10 20 30
M² →
d²σ/dt dM² [mb/(GeV)⁴]
XBL7011-4135

Fig. 5a

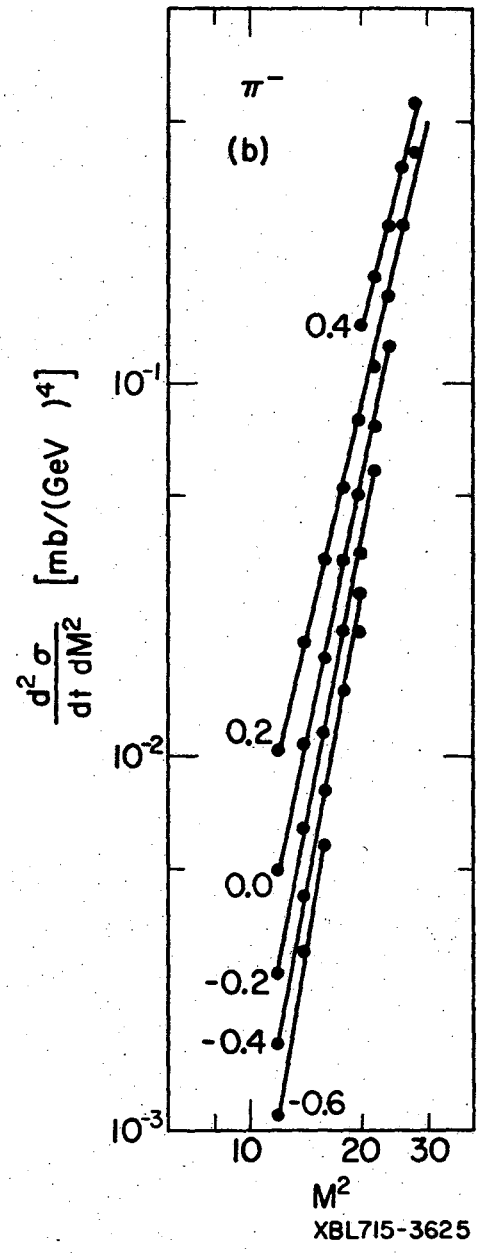
π⁻
(b)
0.4
0.2
0.0
-0.2
-0.4
-0.6
10⁻¹
10⁻²
10⁻³
10 20 30
M²
d²σ/dt dM² [mb/(GeV)⁴]
XBL715-3625

Fig. 5b

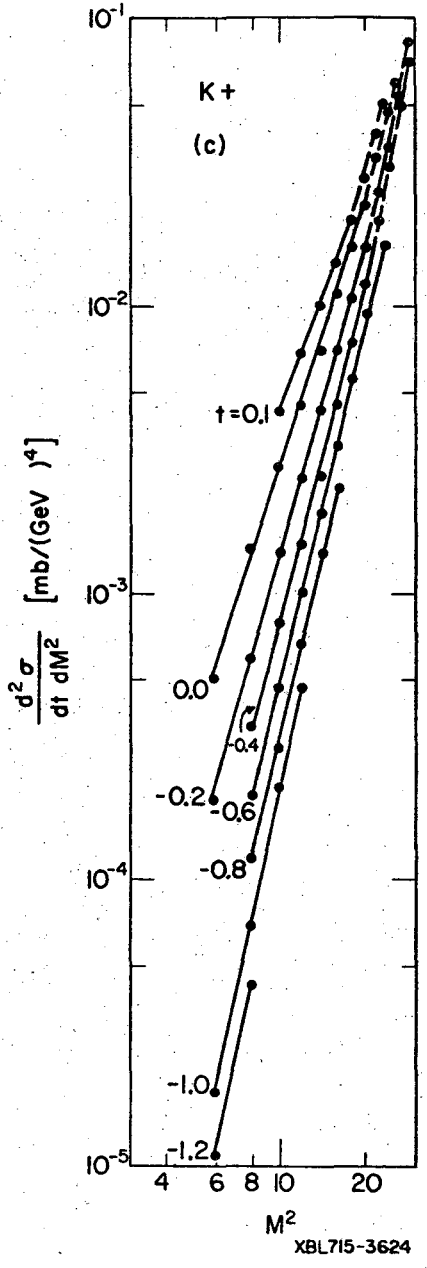
K+
(c)
t=0.1
0.0
-0.2
-0.4
-0.6
-0.8
-1.0
-1.2
$\frac{d^2\sigma}{dt\,dM^2}$ [mb/(GeV)^4]
M^2
XBL715-3624

Fig. 5c

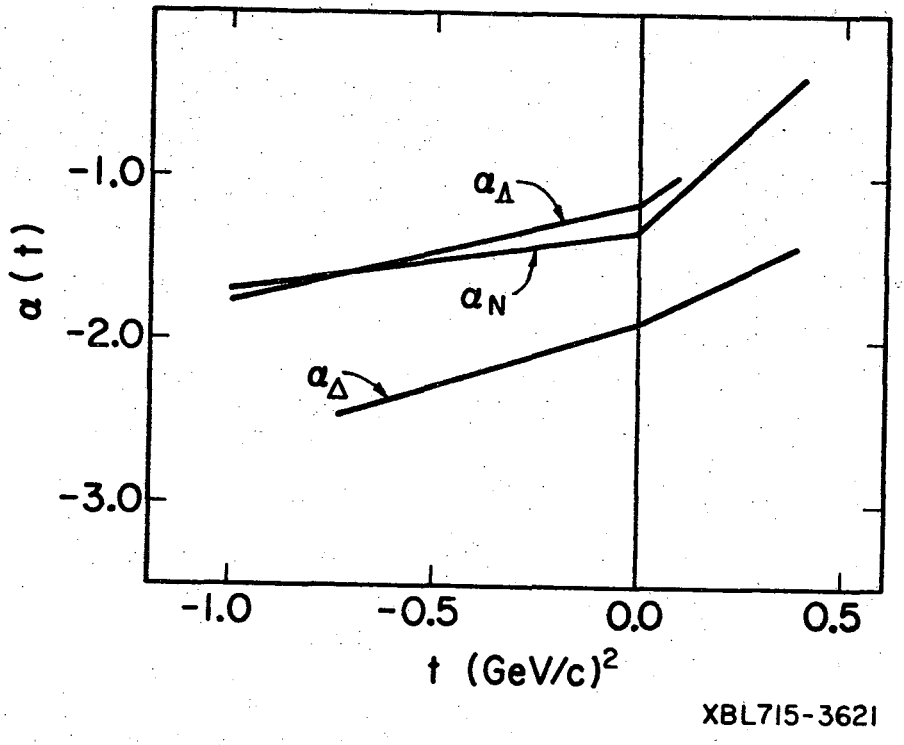
α_Λ
α_N
α_Δ
$\alpha(t)$
t (GeV/c)^2
XBL715-3621

Fig. 6

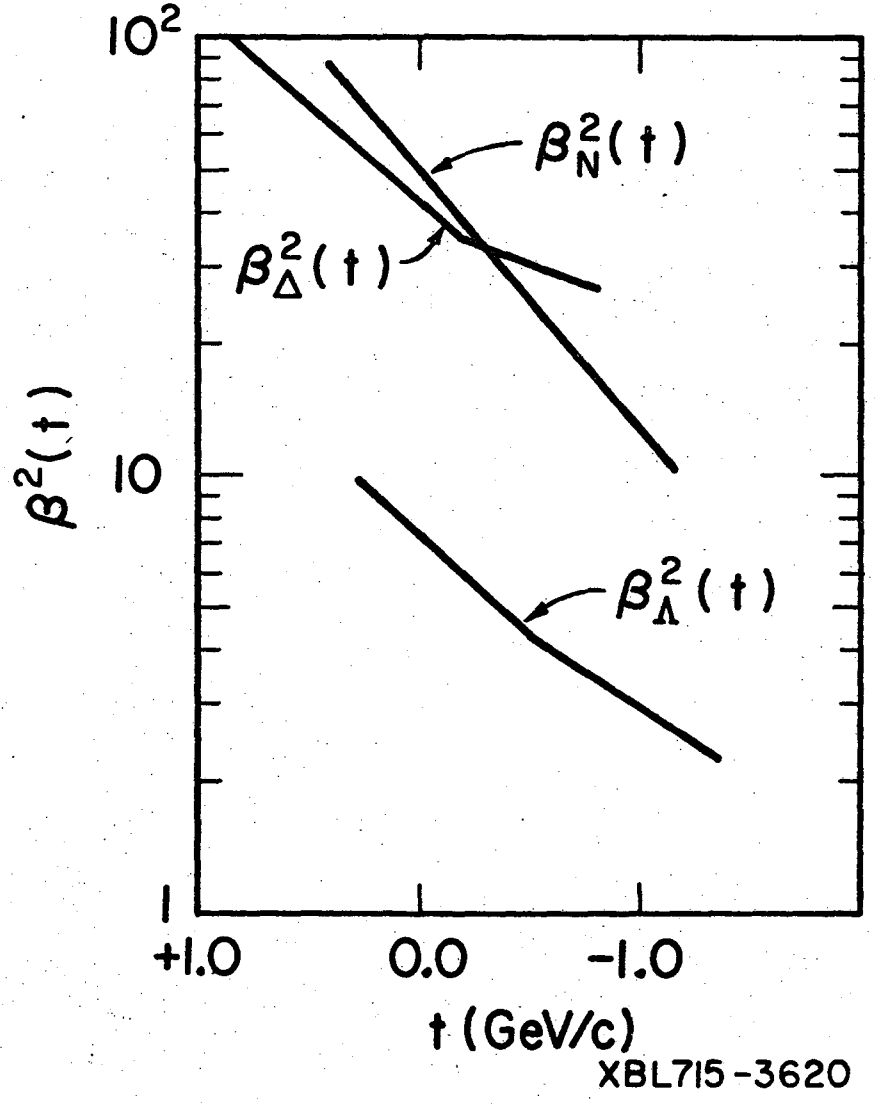
10^2
10
1
$\beta^2(t)$
$\beta_N^2(t)$
$\beta_\Delta^2(t)$
$\beta_\Lambda^2(t)$
+1.0
0.0
-1.0
t (GeV/c)
XBL715-3620

Fig. 7

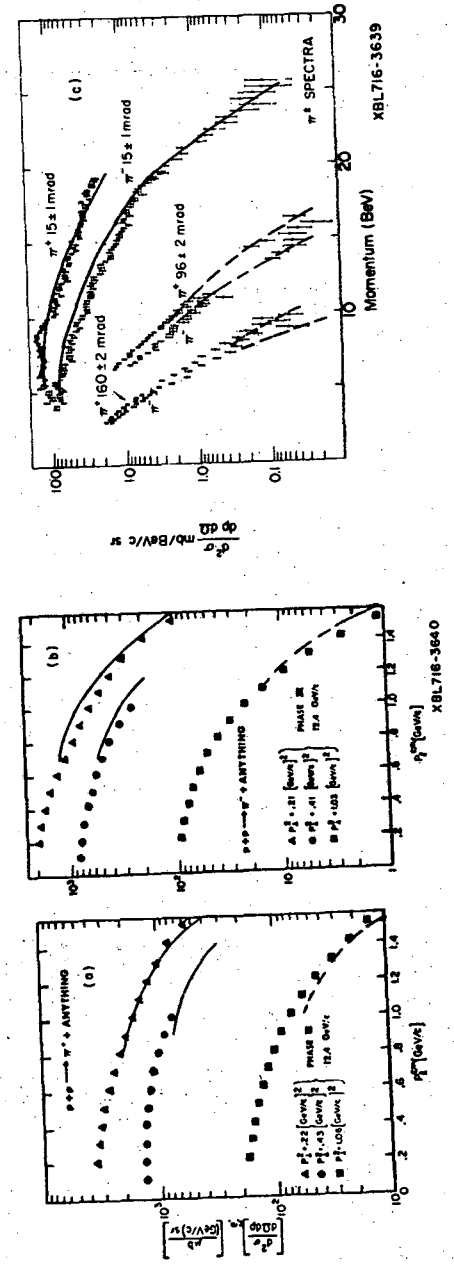
(c)
π^+ SPECTRA
π^+ 15 ± 1 mrad
π^- 15 ± 1 mrad
π^+ 160 ± 2 mrad
π^+ 96 ± 2 mrad
Momentum (BeV)
XBL716-3639
(b)
XBL716-3640
(c)

Fig. 8

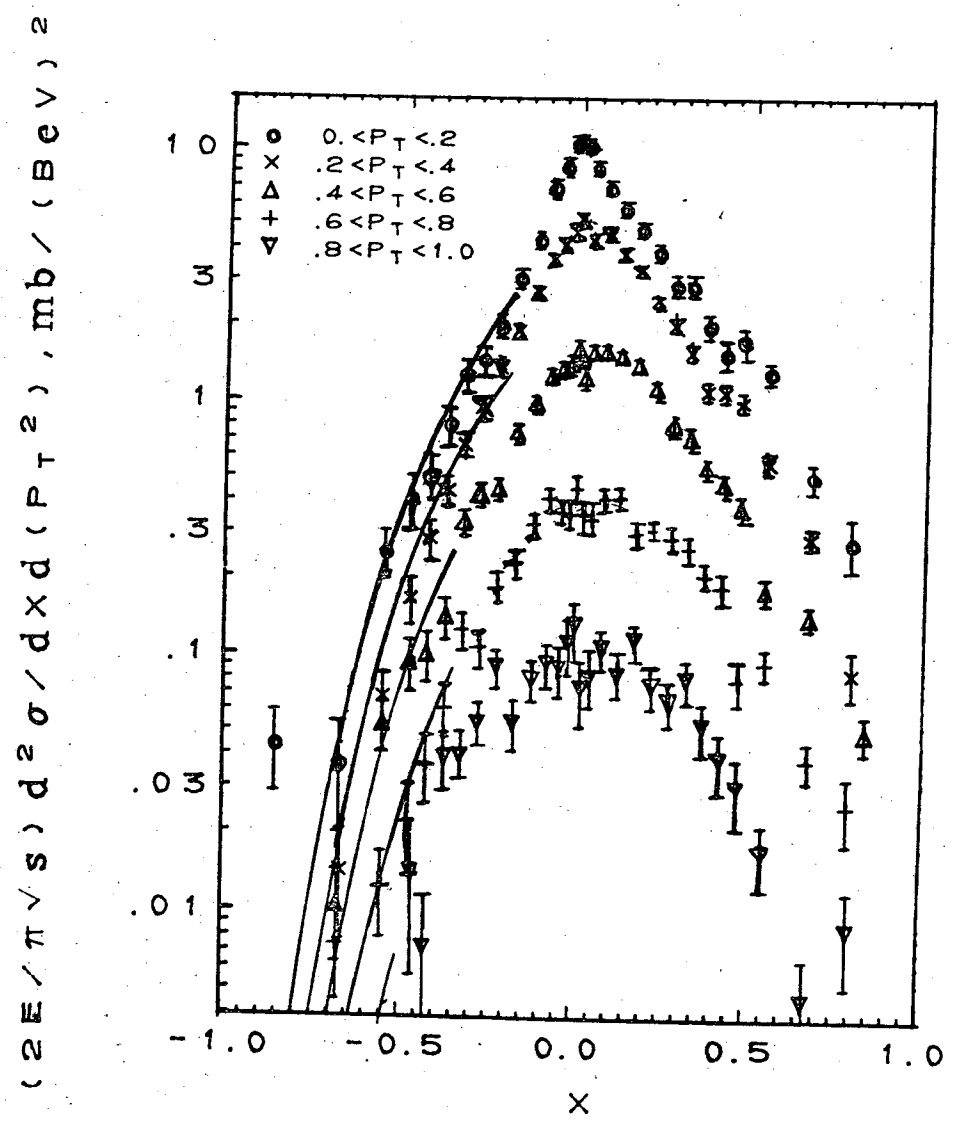

XBL 712-2888A

Fig. 9

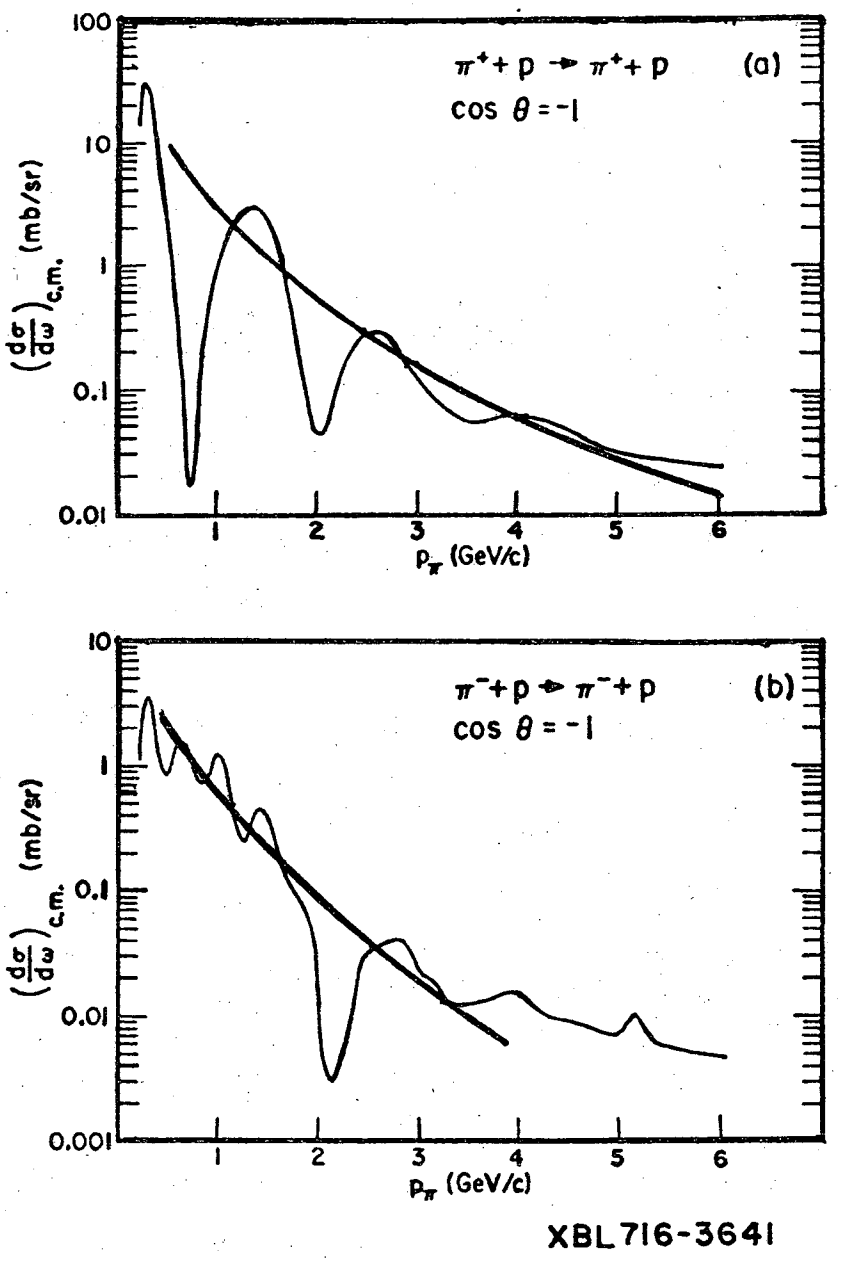

XBL716-3641

Fig. 10a,b

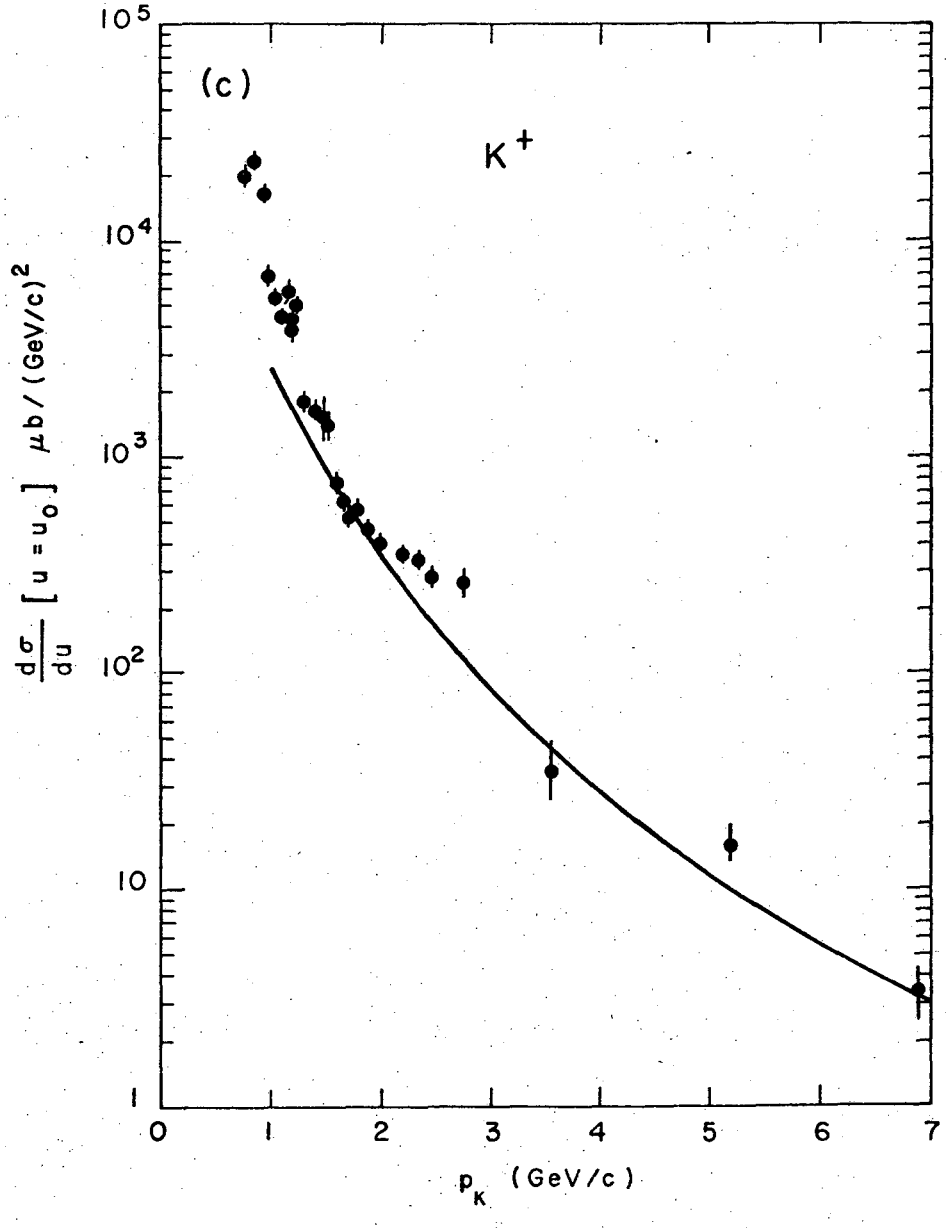

Fig. 10c

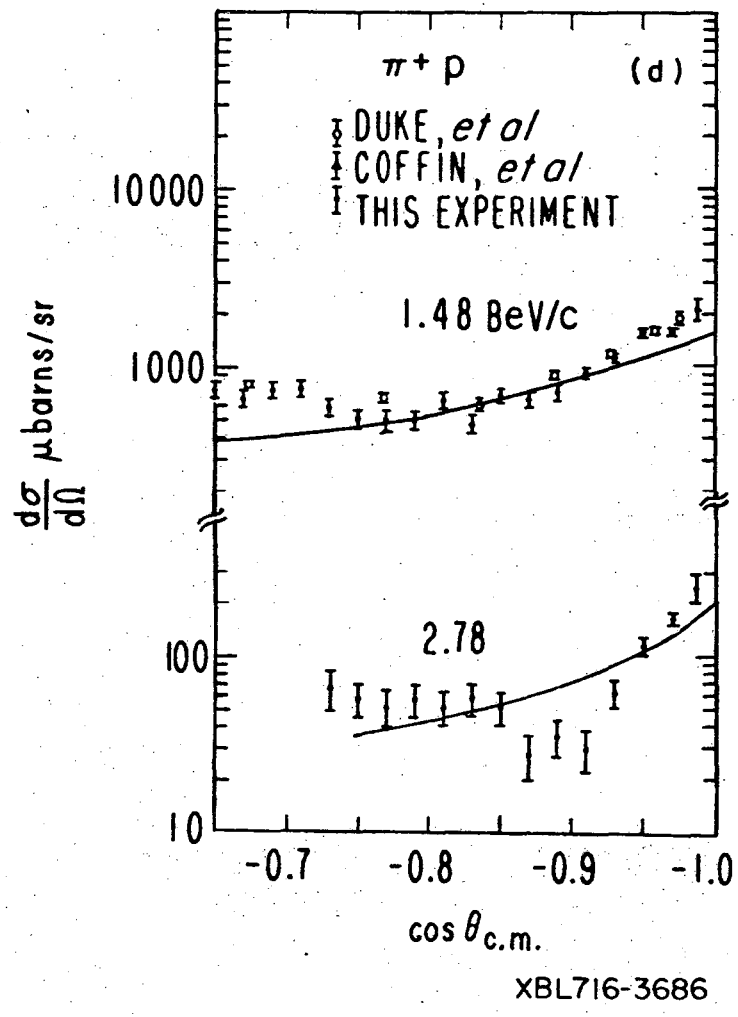

Fig. 10d

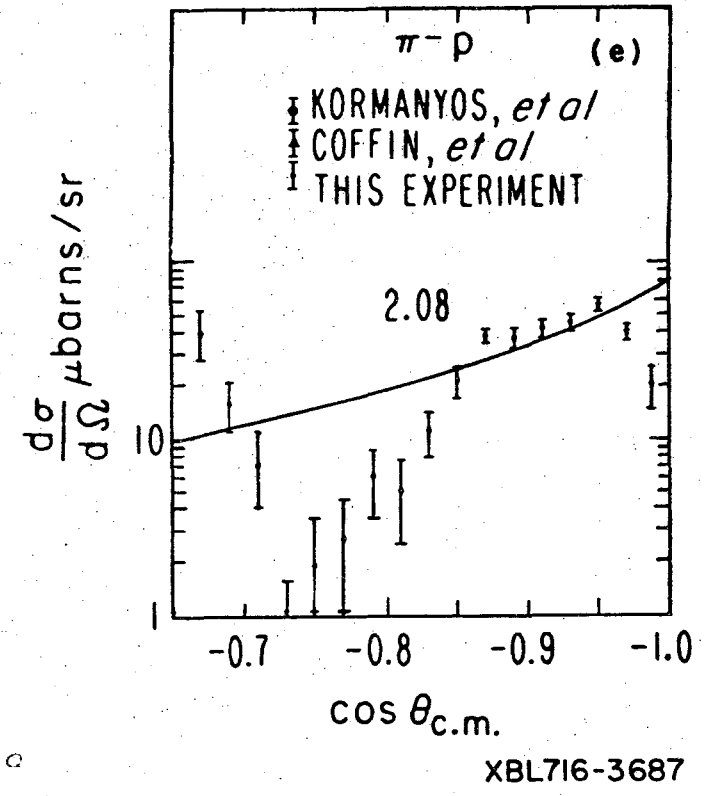

Fig. 10e

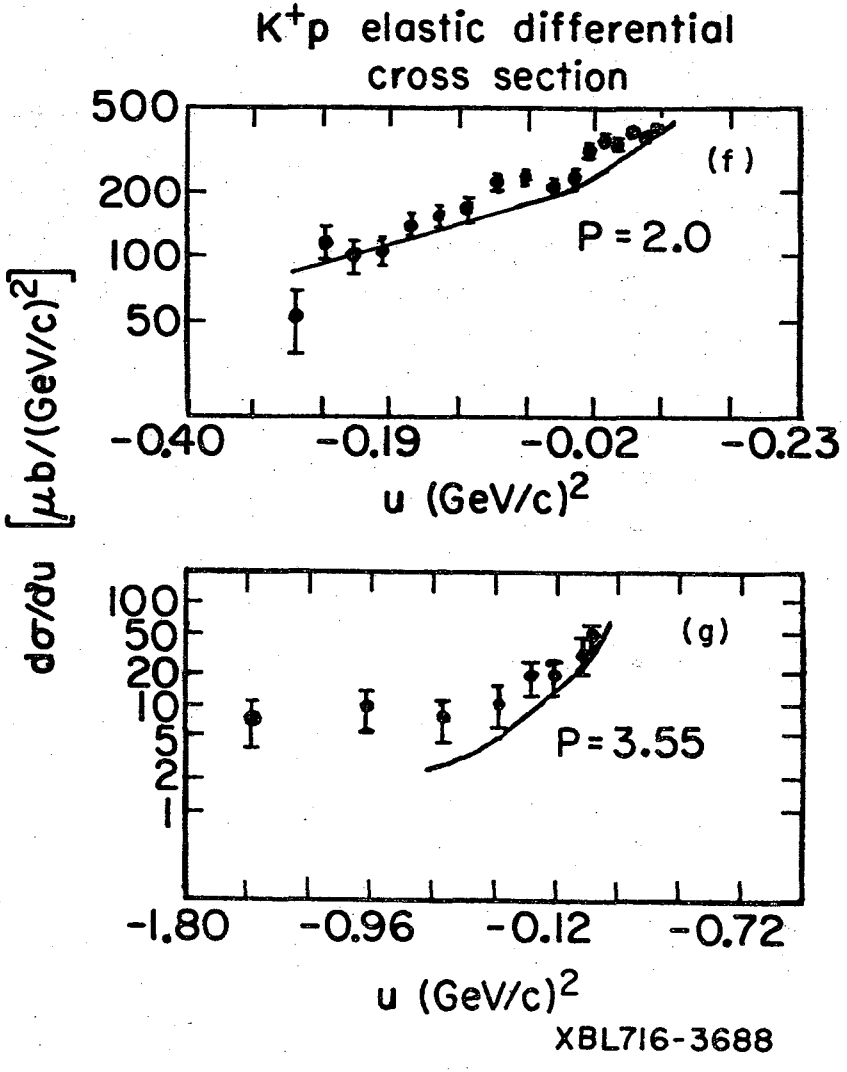

Fig. 10f,g

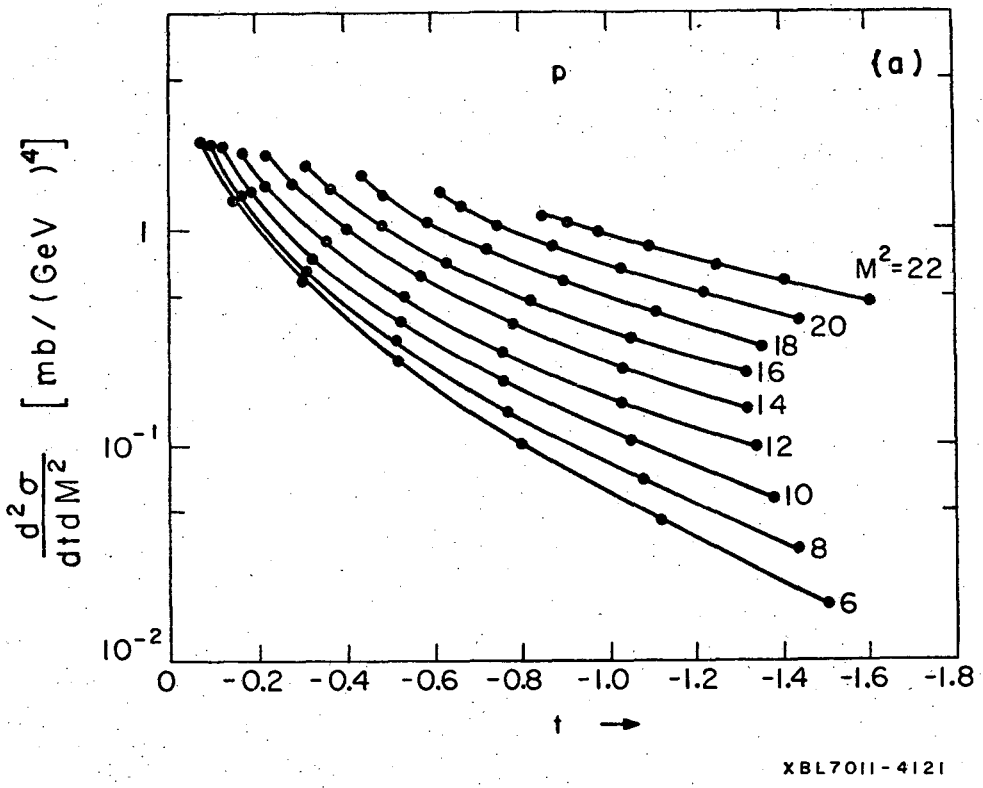

Fig. 11a

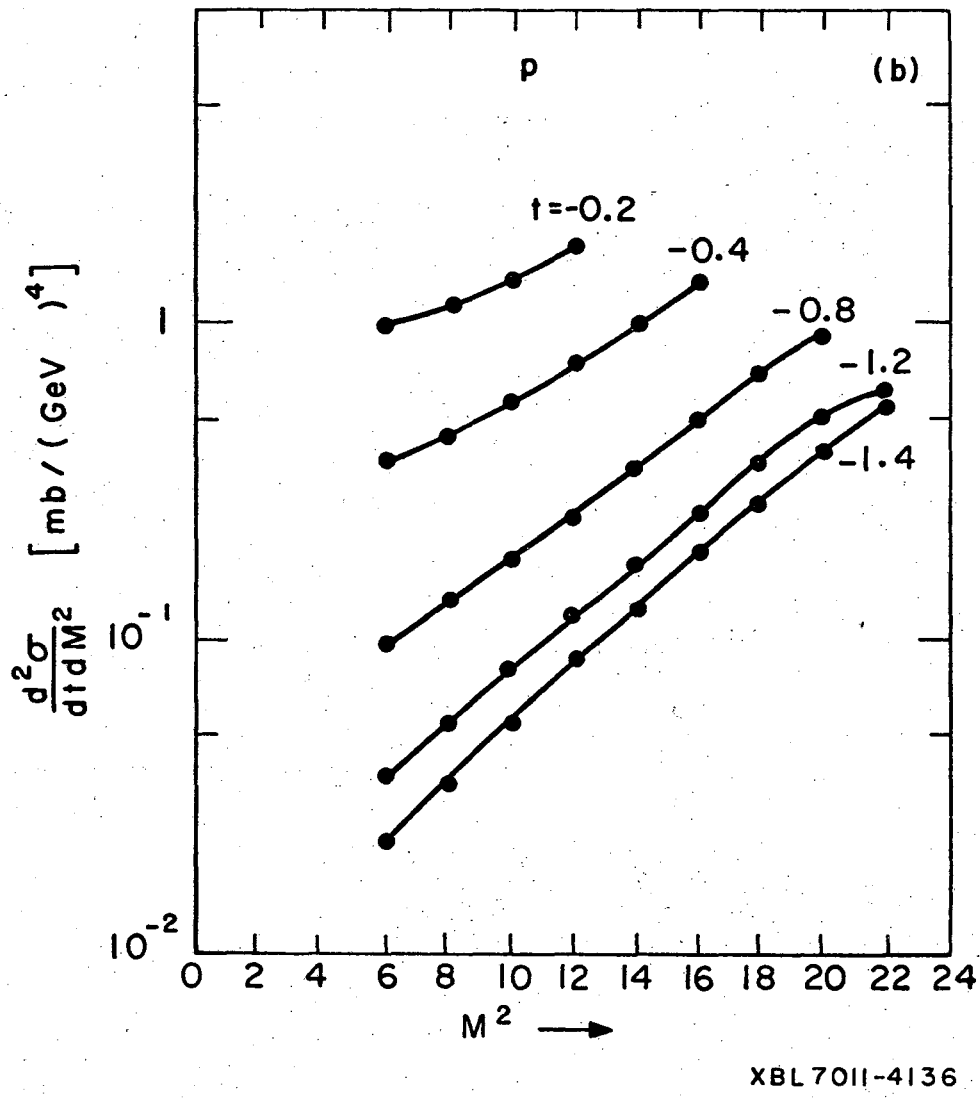

Fig. 11b

LEGAL NOTICE

This report was prepared as an account of work sponsored by the United States Government. Neither the United States nor the United States Atomic Energy Commission, nor any of their employees, nor any of their contractors, subcontractors, or their employees, makes any warranty, express or implied, or assumes any legal liability or responsibility for the accuracy, completeness or usefulness of any information, apparatus, product or process disclosed, or represents that its use would not infringe privately owned rights.

TECHNICAL INFORMATION DIVISION
LAWRENCE BERKELEY LABORATORY
UNIVERSITY OF CALIFORNIA
BERKELEY, CALIFORNIA 94720